Elsevier Editorial System(tm) for Fuel Processing Technology
Manuscript Draft

Manuscript Number: FUPROC-D-16-00002R2

Title: Pseudo-component thermal decomposition kinetics of tomato peels via isoconversional methods

Article Type: Research Article

Keywords: Kinetic analysis; Pyrolysis; Torrefaction; Agro-industrial residues; Isoconversional method; Deconvolution.

Corresponding Author: Dr. Paola Brachi, Ph.D. Student in Chemical Engineering

Corresponding Author's Institution: University of Salerno

First Author: Paola Brachi, Ph.D. Student in Chemical Engineering

Order of Authors: Paola Brachi, Ph.D. Student in Chemical Engineering; Francesco Miccio; Michele Miccio; Giovanna Ruoppolo

***Detailed Response to Reviewers**

REBUTTALS to the 2nd review of the proposed manuscript

Pseudo-component thermal decomposition kinetics of tomato peels via isoconversional methods

by Brachi et al.

The authors would like to thank the reviewers again for their remarks, especially when they provided a detailed analysis of the manuscript, which resulted very helpful in improving the overall quality of the present 2nd revision of the manuscript.

Corrections, modifications and new text additions appear in red color both in the revised manuscript and here.

Discussion about Reviewers' queries and specific replies to distinct points raised by the Reviewers appear in blue color here only.

Reviewer #1

Q1 The kinetics of the thermal decomposition of tomato peel residues under nitrogen atmosphere was studied by non-isothermal thermogravimetric analysis in the heating rate range 2-40 °C/min in this manuscript. Authors assume there are 7 to 8 main pseudocomponents such as cellulose, hemicellulose,lignin,lipids, oil, etc.(line 256-258) According Table 1, the content of cellulose,hemicellulose and lignin is about 95%. So the DTG peak of this three pseudocomponents should be much more bigger than the other pseudocomponents. But the results in Fig 2 and Fig 3 seemed the same for the DTG curve of the 7 pseudocomponents. This is the biggest error. I can not suggest the acceptance of this manuscript in FPT.

The Authors disagree with the Reviewer's remark and do believe that it is simply the result of some misunderstanding. This is extensively explained in the below items.

1. In lines 284-287 of the revised Manuscript, the Authors clearly stated that the pyrolysis of tomato peels is a multistage process that can be modeled by assuming independent parallel reactions corresponding to the decomposition of seven pseudo-components termed as A, B, C, D, E, F and G. However, they did not intend and never identified these pseudo-components with actual tomato peel organic components;
2. In lines 256-259 the Authors only stated that "*The complicated thermal behavior exhibited by tomato peels (experimentally more complex with respect to a conventional woody biomass) is a likely consequence of its very complex chemical composition, which is characterized by the presence of several macro-components (i.e., cellulose, hemicelluloses and lignin, see Table 1) and minor constituents (e.g., lipids, waxes, proteins, oil, etc.) in different percentages [27, 28]*".
3. In lines 260-264 the Author attempted to interpret some thermogravimetric thermal events (i.e., DTG peaks) and not pseudo-components on the basis of both the DTG peak onset temperatures and the typical thermal decomposition temperature of cellulose and hemicellulose as follows

> "*the negligible weight loss (i.e., approximately 7 % wt.) observed at a temperature lower than 200 °C can be attributed to the removal of moisture and to the start of polysaccharides hydrolysis [11] whereas the second and third decomposition stage can be most likely ascribed to the thermal degradation of hemicelluloses and cellulose. Hemicelluloses typically decompose in the 160-360 °C range, while cellulose degrades at higher temperature, i.e., 240-390 °C [11]*". However, in lines 264-267, they also said: "*A clear attribution of all the decomposition events or peaks to a specific chemical species appeared to be hardly achieved when analyzing the DTG profiles only,v because mass losses of several minor chemical components probably occurred during each step at the same time*". Anyway, in this section "3.1 Thermogravimetric analysis" of Manuscript no mention was made to pseudo-components.

The following further information could be useful in helping the Reviewer to better interpret the Authors' points.

The notation of "pseudo-components" was introduced by Di Blasi (2008)[1] just to emphasize that on differential TG curves, each zone (e.g. peaks, shoulders, gently sloping baseline) attributed to a pseudo-component reflects the contribution of a main biomass component (e.g., hemicellulose, cellulose, lignin and extractives) to the total weight loss of the sample. This nevertheless does not exclude some participation of other biomass constituents to an extent that depends on the biomass characteristics and the severity of the conversion conditions.

The number of pseudo-components used in the majority of the kinetic approaches is three[2], while in a few cases the contribution of extractives and oily fractions or more than one reaction stage in the decomposition of hemicellulose and/or lignin is also taken into account[3]. The fraction of the extractives is not often found in literature works, and sometimes it is added to that of the hemicellulose.[1] As for this latter component, sometimes it is added to the cellulose, and only the holocellulose fraction is indicated.[1]

This clearly would explain why it makes no sense to compare the quantitative data on the polymeric composition of tomato peels reported in Table 1 with the pseudo-component contributions to the total mass loss as expressed by the ratio of the area under the "pseudo-component peak" to the total area under the DTG curve (cf. Eq. 13).

Anyhow, in the Manuscript, an attempt was made by the Authors to identify (qualitatively and not quantitatively) the "main contributors" of each pseudo-component on the basis of the E_α-values obtained for these latter by the application of isoconversional methods (cf. lines 301-317), also to comply with the request previously posed by the Reviewer #2 at the point **Q17**. For example, since the values of the apparent activation energies (E_α vs. α) obtained for pseudo-component B and C were found consistent with the values reported in literature for hemicellulose (80-116 kJ/mol) and cellulose (195-286 kJ/mol), respectively [23, 24], the "main contributor" of the pseudo-component

---

[1] C. Di Blasi, Modeling chemical and physical processes of wood and biomass pyrolysis, Prog. Energ. Combust. 34 (2008) 47-90.

[2] E. Biagini, L. Tognotti, A Generalized Procedure for the Devolatilization of Biomass Fuels Based on the Chemical Components, Energ. Fuel 28 (2014) 614−623.

[3] V. Mangut., E. Sabio, J. Ganàn, J.F. Gonzalez, A. Ramiro, C.M. Gonzàlez, S. Romànan, A. Al-Kassir, Thermogravimetric study of the pyrolysis of biomass residues from tomato processing industry, Fuel Process. Technol. 87 (2006) 109-115.

B and C was identified as hemicellulose and cellulose, respectively. However, some participation of other biomass constituents is not to be excluded, for instance lignin whose decomposition is known to take place in the temperature range from 160 to 900 °C at a very low mass rate[4]. The same was made for the other pseudo-components (see lines 307-317 of the revised Manuscript).

---

[4] H. Yang, R. Yan, H. Chen, D.H. Lee, C. Zheng, Characteristic of hemicellulose, cellulose and lignin pyrolysis, Fuel, 86 (2007), 1781–1788.

Reviewer #2

Q 1: Authors nicely improved the manuscript. The agreement with the corrected results for the 60 K/min has been improved, also the new results for 80 K/min are in even better agreement with the results of simulations. Interestingly, the simulated curves in Fig. 5 look even too complex in comparison with the experimental results. It seems like the simulated curves were composed from too many peaks - which is in fact true because adopted methodology is based on the symmetrical functions (to describe asymmetrical shape) … Thus, in my opinion, it is essential to apply the methodology based on the asymmetrical functions, and compare the results.

The Authors believe that a comparative study on the effects that different deconvolution functions, in particular the asymmetric ones, may have on the kinetic data arising from the proposed analytical approach falls out of the scope of the Manuscript that only deals with a more practical task, as clearly stated in Lines 67-68 "*to propose a set of reliable kinetic parameters for future design and optimization of thermochemical processes involving tomato peel feedstock*".
The Authors do believe that the comparative study would deserve such an attention and imply such a work to lead them to another "companion paper".

Q 2: It is also supported by the interesting discussion on the possible origin of the peaks, where duplications are observed.

Note that the abovementioned duplications trivially arose from a typing error that the Authors have detected and corrected the present 2nd revision of the manuscript. In particular, they had wrote D instead of C in line 305 of the previous revised Manuscript.

Few detail comments:

Q 4: L167: add reference to the Mathworks File Exchange website.

This has been done.

Q 5: L164, L22, I would avoid phrases like „open-source Matlab functions", since Matlab is a commercial code, please replace it with „freely available" or similar.

This has been done.

Q 4: Fig. 1. Dots are still barely visible. Use dark color for dots.

This has been done.

Highlights

1. Thermal behavior and decomposition kinetics of tomato peels were studied by TGA.
2. The deconvolution of individual processes from complex DTG curves was explored.
3. Model-free kinetic analysis provided a way to bypass the unknown reaction models.
4. A conversion-dependent activation energy was obtained for each deconvoluted peak.
5. The predictive ability of the evaluated kinetic parameters was demonstrated.

*Manuscript
Click here to download Manuscript: REVISED_Manuscript_Brachi et al..docx Click here to view linked References

Pseudo-component thermal decomposition kinetics of tomato peels via isoconversional methods

Paola Brachi[a1], Francesco Miccio[b], Michele Miccio[a] and Giovanna Ruoppolo[c]

[a]*Department of Industrial Engineering, University of Salerno, via Giovanni Paolo II 132, 84084 Fisciano (SA), Italy*

[b]*Institute of Science and Technology for Ceramics (ISTEC-CNR), via Granarolo 64, 48018 Faenza (RA), Italy*

[c]*Institute for Research on Combustion, National Research Council, P.leTecchio 80, 80125 Napoli, Italy*

Abstract

The kinetics of the thermal decomposition of tomato peel residues under nitrogen atmosphere was studied by non-isothermal thermogravimetric analysis in the heating rate range 2-40 °C/min. Due to the complexity of the kinetic mechanism, which implies simultaneous multi-component decomposition reactions, an analytical approach involving the deconvolution of the overlapping decomposition steps from the overall differential thermogravimetric curves (DTG) and the subsequent application of model-free kinetic methods to the separated peaks was employed. Two freely available Matlab functions, which adopt a non-linear optimization algorithm to decompose a complex overlapping-peak signal into its component parts, were used. Different statistical functions (i.e., Gaussian, Voigt, Pearson, Lorentzian, equal-width Gaussian and equal-width Lorentzian) were tested for deconvolution and the best fits were obtained by using suitable combinations of Gaussian and Lorentzian functions. For the kinetic analysis of the deconvoluted DTG peaks, the Friedman's isoconversional method was adopted, which does not involve any mathematical approximation. The reliability of the derived kinetic parameters was proved by successfully reproducing two non-isothermal conversion curves, which were recorded at a heating rate of 60 °C/min and 80 °C/min and not included in data set used for the kinetic analysis. Seven pseudo-components were identified

---

[1] Corresponding author. Tel.: +39 089 964067; e-mail address: pbrachi@unisa.it
E-mail addresses: miccio@irc.cnr.it (F. Miccio), mmiccio@unisa.it (M. Miccio), ruoppolo@irc.cnr.it (G. Ruoppolo).

as a result of the deconvolution procedure and satisfactorily associated with the main constituents of the investigated tomato peels.

Keywords: Kinetic analysis, Pyrolysis, Torrefaction, Agro-industrial residues, Isoconversional method, Deconvolution.

1. Introduction

Tomato (Lycopersicon esculentum) is the second most important vegetable crop next to potato. Nowadays, about 150 million tons are produced and consumed each year all over the world, of which 40 million as processed products (i.e., tomato paste, peeled or unpeeled, whole or unwhole tomatoes) [1]. During tomato processing, two residual fractions, which represent 3% to 5 % by weight of the whole tomato, are typically generated: i. tomato peels, which are the by-product of the peeling of tomatoes used for canning and ii. tomato pomace, which is a mixture of the tomato peels, crushed seeds and small amounts of pulp that remain after the processing for juice, soup, or ketchup [2].

In keeping with the internationally agreed waste management strategies (DIRECTIVE 2008/98/EC), research interest in the conversion of tomato processing residues into useful form of bioenergy and/or biofuels through different thermal conversion processes (i.e., torrefaction [3, 4], pyrolysis [5] and hydrothermal carbonization [6]) has increased significantly in the last years.

The thermal decomposition (e.g., pyrolysis) plays a crucial role in all of the thermochemical conversion processes and mastering qualitative characteristics and quantitative kinetics of this step is essential to design and control a thermal conversion unit. However, to the best of our knowledge, there is only one work by Mangut et. al [5] in the literature addressing the kinetic analysis of the complex thermal decomposition of tomato residues (i.e., tomato seeds and/or tomato peels), which involves several and also simultaneous steps. Specifically, a multi-component model-fitting approach was employed in the above investigation to estimate kinetic parameters (i.e., activation energy, pre-exponential factor and reaction order) from non-isothermal TGA data. However, no attempts were made by the cited authors [5] to validate the computed kinetic parameters, despite the fact that it is widely recognized that model-fitting methods produce highly uncertain kinetic parameters, especially from dynamic thermogravimetric data [7, 8]. In other words, non-unique solutions are usually found as a result of the fitting procedure in dynamic conditions, which is due to the so-called compensation effect [7]. As a consequence, the derived kinetic parameters may have no practical value in predicting the behavior of such a feedstock in order to design and control a dedicated thermal conversion plant.

With this background, the primary aim of the present investigation was to provide new insights into the thermal decomposition kinetics of tomato peels under non-isothermal conditions and to propose a set of reliable kinetic parameters for future design and optimization of thermochemical processes involving tomato peels as a feedstock. In order to overcome the aforementioned problems associated with model-fitting methods [7, 9], a model-free kinetic approach based on the isoconversional method of Friedman [10] was selected to analyze data from non-isothermal thermogravimetric measurements. As the name implies, model-free techniques do not require any previous knowledge or assumption of the kinetic model and yield kinetic parameters as a function of either temperature (non-parametric kinetics) or conversion (isoconversional analysis) [11]. However, since it has been proved that model-free methods do provide incorrect kinetic results for datasets containing overlapping peaks [12], i.e., data from processes involving independent and simultaneous multiple-component reactions (as it is the case for the thermal decomposition of tomato peels), an analytical approach implying the separation of the overlapping peaks from the overall differential thermogravimetric curves (DTG curve) and the subsequent kinetic analysis of the separated decomposition steps was adopted.

This paper represents the first successful application of a model free kinetic approach to the thermal decomposition of tomato peels. Therefore, it demonstrates novelty in extending the application of model-free isoconversional methods, most commonly used for the kinetic analysis of thermally simulated process involving polymers [13] or other complex organic compounds [14], also in the field of biomass thermochemical conversion processes, with particular reference to a scarcely investigated agro-industrial residual biomass (i.e., tomato peels).

2. Materials and Methods

2.1 Feedstock sampling and characterization

Tomato peels (TPs) used in this work were collected from a tomato processing industry located in Salerno (40°47'24.5"N, 14°46'15.8"E), Campania region (ITA), in September 2014. In order to preserve their original state and prevent microbial degradation, all samples were stored in an air-tightened plastic bag at -20 °C. Prior to use, the raw material was first conditioned to 6 % wt. moisture content by leaving it at ambient temperature for 48 h in a laboratory fume hood and then ground in a batch knife mill (Grindomix GM 300 by Retsch) for 3 min at a speed as high as 3200 rpm. The milled TPs were then sieved and the 0-400 μm size fraction was selected for the subsequent analysis.

Proximate (TGA 701 LECO thermogravimetric analyzer), ultimate (CHN 2000 LECO and SC 144 DR LECO analyzer) and calorific (Parr 6200 Calorimeter) analyses were performed in order to obtain the basic properties of tomato peels as a fuel. All these analyses were performed in duplicate at least. The average values and the related standard deviations are reported in Table 1.

The main polymeric components (i.e., hemicellulose, cellulose and lignin) of raw TPs were determined according to the procedure by Rowell et al. [15]. In accordance with Laboratory Analytical Procedures (LAP) established by National Renewable Energy Laboratory (NREL) [16], samples of air-dried TPs passing a 40 mesh screen were first submitted to Soxhlet extraction with an ethanol/toluene (1:2, v:v) solution in order to remove the extractives (i.e., fats, resin, wax, phenol, pigments, oils and other organic compounds), which could affect the subsequent analysis of polymer composition. The extraction was conducted for 24 hours at the rate of about 8 siphon cycles per hour. The resulting oven-dried extractive-free sample was then submitted to a delignification process by treating it with sodium chlorite ($NaClO_2$, technical grade, 80 %) and acetic acid (reagent grade) for 6 h in a water bath at 70 °C. The extractive- and lignin-free white holocellulose sample was subsequently treated with sodium hydroxide (17.5 % and 8.3 % wt.) and acetic acid (10 % wt.) solutions in order to isolate the α-cellulose fraction. The soluble fraction remaining after this treatment represented hemicelluloses. The lignin content was calculated by difference. The polymeric composition, based on the above procedure, is also shown in Table 1.

2.2 Experimental techniques

Non-isothermal decomposition kinetics of tomato peels were studied by means of thermogravimetric technique (TGA/DTG). The experiments were carried out in a TA Instruments analyzer Q600 SDT under linear heating conditions. The sample holder was an open-type alumina pan. Low sample masses (~ 10 mg) and small particle sizes (< 400 μm) were selected in order to reduce the effect of intra-particle mass and heat transport limitations and thus avoid problems of "thermal lag" between the sample and the controlling (external) thermocouple during the tests. Nitrogen was used as purge gas at a flow rate of 100 ml/min to ensure an inert atmosphere and to prevent secondary reactions by volatiles produced during the solid thermal decomposition. The temperature was controlled from room temperature up to about 1000 °C at seven different heating rates (2, 5, 10, 20, 40, 60 and 80 °C/min). Variations of the sample residual mass with respect to time and temperature (TG data) and its time derivative (DTG data) were collected simultaneously during each test by using Q600 Software and then analyzed according to the method described in the next section.

2.3 Theoretical background

Isoconversional methods take their origin in the following single-step kinetic equation:

$$\frac{d\alpha}{dt} = A\, exp\left(-\frac{E}{RT}\right) \cdot f(\alpha) \qquad (1)$$

where A and E are kinetic parameters, namely the pre-exponential factor and the apparent activation energy, respectively, R is the gas constant, T the absolute temperature, f(α) the reaction model and α the reacted fraction of the sample (or conversion degree), which is defined by the following Eq. (2):

$$\alpha = \frac{W_0 - W_t}{W_0 - W_f} \qquad (2)$$

where W_t, W_0 and W_f are the sample mass at a given time t, at the beginning and at the end of the mass event of interest, respectively.

All isoconversional methods rely on the fact that the reaction rate at a constant extent of conversion is only a function of the temperature, as merely results from having taken Eq. (1) to describe the rate of solid-state reactions. In more details, these methods make use of the temperature dependence of the isoconversional rate to evaluate the isoconversional value of the activation energy, E_α, without any previous knowledge or particular assumption of the reaction model [8]. This is the reason why isoconversional methods are also called “model-free” methods and it can be easily demonstrated by taking the derivative of the logarithm of the reaction rate (Eq. (1)), at α = cost, which returns:

$$\left[\frac{\partial ln\,(d\alpha/dt)}{\partial T^{-1}}\right]_\alpha = -\frac{E_\alpha}{R} \qquad (3)$$

Typically, to experimentally obtain the temperature dependence of the isoconversional rate, a series of 3-5 runs at different heating rates or a series of runs at different constant temperature are performed [8].

For a multi-component kinetic analysis of a reacting solid, the previous single step kinetic equation Eq. (1) becomes:

$$\frac{d\alpha}{dt} = \sum \gamma_j \frac{d\alpha_j}{dt} = \sum \gamma_j\, A_j\, exp\left(-\frac{E_j}{RT}\right) f\left(\alpha_j\right) \qquad (4)$$

where γ_j is the ratio of the mass loss of the jth pseudo-component to the total sample mass loss, which must fulfill the following relationships:

$$\sum \gamma_j = 1 \qquad (5)$$

$$\sum \gamma_j . \alpha_j = \alpha \qquad (6)$$

A detailed derivation of Eqs. (4-6) can be found in [17].

2.4 Separation of independent overlapping pseudo-component decomposition reactions

The separation of the independent and overlapping pseudo-component reactions from the set of experimental DTG curves at the different heating rates of 2, 5, 10, 20, 40 °C/min was performed by means of two different Matlab m-functions, namely ipf.m and peakfit.m (Copyright (c) 2014, 2015 Thomas C. O'Haver). These m-functions use a non-linear optimization algorithm to decompose a complex overlapping-peak signal into its component parts and they are available free of charge on the Mathworks File Exchange website [18]. Different conventional statistical distribution equations (i.e., Gaussian, Voigt, Pearson, Lorentzian, equal width Gaussian and equal width Lorentzian), included as standard functions in the above mentioned Matlab m-functions, were tested for the deconvolution and the best fits were obtained by using a suitable combination of Gaussian and Lorentzian peak-shape functions, described by the following Eqs. (7) and (8), respectively:

$$y = y_o + \frac{S}{w\cdot\sqrt{\frac{\pi}{2}}}\exp\left[-\frac{2(x-x_o)}{w^2}\right] \qquad (7)$$

$$y = y_o + \frac{2S}{\pi}\cdot\frac{w}{4(x-x_0)^2+w^2} \qquad (8)$$

where y_o is the baseline offset, S the total area under the curve from the baseline, x_0 the center of the peak and w the width of the peak at half height. Specifically, to separate the different decompositions stages, the experimental DTG data were first loaded into the ipf.m function, which provided the best-fit description of the experimental curve by varying the number, the position, the shape and the width of discrete peaks at each heating rate. Then, the determination of fitting parameters (i.e., y_o, S, w, x_o) and of the model error was performed by using the peakfit.m function.

2.5 Pseudo-component kinetic analysis

The Friedman's differential isoconversional method was employed to determine the dependence of the activation energy on the conversion degree for each of the pseudo-components resulting from the peak deconvolution procedure. The method is based on the following Eq. (9):

$$ln\left(\frac{d\alpha_j}{dt}\right)_{\alpha_{j,i}} = ln\left[\beta_i\left(\frac{d\alpha_j}{dT}\right)_{\alpha_{j,i}}\right] = \ln\left[A_{\alpha_j} f\left(\alpha_j\right)\right] - \frac{E_{\alpha_j}}{RT_{\alpha_{j,i}}} \tag{9}$$

which can be easily derived by computing the natural logarithms of the Eq. (1). The subscripts i and j were introduced to denote the investigated heating rates and the different pseudo-components, respectively. $T_{\alpha j,i}$ is the temperature at which the extent of conversion α_j is reached under the ith heating rate, β_i.

$E_{\alpha j}$ values were computed varying α_j in the range of 0.05 to 0.95 with a step of 0.05. To this end, the deconvoluted DTG data (dW_j/dt vs. T) were at first converted in TG data (W_j vs. T) using the Euler's forward method [19]. Then, the TG data were converted to the plot of the conversion degree versus temperatures (α_j vs. T) by means of the Eq. (10):

$$\alpha_j = \frac{W_{j0} - W_{jt}}{W_{j0} - W_{jf}} \tag{10}$$

where W_{jt}, W_{j0} and W_{jf} are the mass of the jth pseudo-component at a given time t, at the beginning and at the end of the mass event of interest, respectively. For each of the 19 conversion levels (α_j) considered in the range 0.05-0.95, the experimental value of the conversion rate, $(d\alpha_i/dt)_{\alpha i,j}$, was determined by using the Eq. (11)

$$\left(\frac{d_{\alpha_j}}{dt}\right)_{\alpha_{j,i}} = -\left(\frac{dW_{jt}}{dt}\right)_i \frac{1}{\left(W_{j0} - W_{jf}\right)_i} \tag{11}$$

Finally, for any given α_j, the value of $E_{\alpha j}$ was calculated from the slope of the straight line graph of $\ln(d\alpha_j/dt)_{\alpha j,i}$ against $1/\ T_{\alpha j,i.}$ (see Eq. 9) at the different heating rates (i.e., 2, 5, 10, 20 and 40 °C/min). Thus, the dependence of $E_{\alpha j}$ on α_j was obtained.

2.6 Validation of the kinetics analysis approach

In keeping with the ICTAC Kinetics Committee recommendations [8, 9], the reliability of the computed kinetic parameters was checked by reproducing two non-isothermal conversion profiles (i.e., at 60 and 80 °C/min) not included in dataset used for the kinetic analysis. To this end, first the conversion profile of the individual pseudo-components (i.e., dependence of α_j on T) was simulated by applying the following equation by Vyazovkin [20]:

$$\frac{1}{\beta}\int_0^{T_{\alpha_j}} exp\left(-\frac{E_{\alpha_j}}{RT}\right)dT = \frac{1}{\beta^*}\int_0^{T^*_{\alpha_j}} exp\left(-\frac{E_{\alpha_j}}{RT}\right)dT \tag{12}$$

where: i. $E_{\alpha j}$ is the value of activation energy at a given α_j, just as obtained from kinetic analysis; ii. $T_{\alpha j}$ is the unknown variable to be found as a solution of Eq.(12) and represents the temperature at which the conversion degree, α_j, will be reached at an arbitrary heating rate, β; and iii. $T^*_{\alpha_j}$ is the temperature at which the conversion degree α_j is experimentally achieved at a given heating rate β^*. In more details, the Eq. (12) was solved numerically applying the trapezoidal rule in a MS Excel® spreadsheet. The experimental values of $T^*_{\alpha_j}$ obtained from dynamic TG curves recorded at β^*= 40 and 60 °C/min were employed to perform the simulation at 60 and 80 °C/min, respectively, i.e., in calculating the integral on the right hand side of the Eq.(12). Finally, the global decomposition curves of tomato peels at the heating rates of 60 and 80 °C/min, were obtained as the weighted sum of the conversion profiles of the individual pseudo-components. The contribution γ_j of the jth pseudo-component to the total mass loss was assumed equal to the average of the values obtained at the five investigated heating rates (i.e. β_i = 2, 5, 10, 20, 40 °C/min) according to the following Eq. (13):

$$\gamma_j = \frac{1}{5}\cdot\sum_i \gamma_i = \frac{1}{5}\cdot\sum_i\left(\frac{S_{j,i}}{\sum_j S_{j,i}}\right) \tag{13}$$

where $S_{j,i}$ is the total area under the DTG curve of the jth pseudo-component at the ith heating rate β_i, as reported in Table 2. The quality of fit between the simulated and experimental curves was evaluated through the average deviation percentage (AVP) proposed by Orfao et al. [21]:

$$AVP = 100\cdot\sqrt{\frac{\sum_{k=1}^{N}\left[(\alpha)_{k,exp}-(\alpha)_{k,calc}\right]^2}{N}} \tag{14}$$

where N is the number of experimental points employed.

3. Results and Discussion

3.1 Thermogravimetric analysis

The TG and DTG curves of the tomato peel residues under nitrogen atmosphere at five different heating rates (i.e., 2, 5, 10, 20, 40 °C/min), are shown in Fig. 1a and Fig. 1b, respectively. The TG curves show the percentage mass loss of tomato peels over the temperature range from room temperature up to about 1000 °C. It can be observed that the actual temperature range from the start to the finish of the tomato peel decomposition is narrower at a lower heating rate with respect to a higher heating rate (Fig. 1a). It also results that higher heating rates are accompanied by higher reaction rates and higher reaction temperatures (i.e., DTG peak temperature shifts to the higher values with increasing heating rates), as shown in Fig. 1b. Moreover, the separation of the DTG peaks is more evident at low heating rates, even though it not clearly revealed in Fig. 1b due to the difference in scale between the different curves. These findings agree with those found in literature for other kinds of biomass [22]. Basically, there are several phenomena that could explain the observed effects of the heating rate on the TG and DTG curve shape and characteristic temperatures, including: i. the time interval in which the sample is exposed to a given temperature decreases as the heating rate increases resulting in higher residual mass [23]; ii. a high heating rate is more likely to generate a temperature difference between the sample and the TGA thermocouple built-in sensor and, hence, the real sample temperature may lag behind that of the thermocouple [24]; iii. a competitive mechanism is established between the endothermic reactions of the primary solid decomposition leading to volatile formation and the exothermic vapor-solid interactions leading to secondary char formation, this latter being favored at low heating rate [25, 26].

Thermogravimetric measurements suggest that the pyrolysis of the investigated tomato processing residue is a rather complex process occurring in several stages as it is clearly reflected by the presence of several DTG peaks (Fig. 1b), which are also reflected in less noticeable changes in the slope of the TG curves. The complicated thermal behavior exhibited by tomato peels is a likely consequence of its very complex chemical composition, which is characterized by the presence of several macro-components (i.e., cellulose, hemicelluloses and lignin, see Table 1) and minor constituents (e.g., lipids, waxes, proteins, oil, etc.) in different percentages [27, 28]. The negligible weight loss (i.e., approximately 7 % wt.) observed at a temperature lower than 200 °C can be attributed to the removal of moisture and to the start of polysaccharides hydrolysis [11] whereas the second and third decomposition stage can be most likely ascribed to the thermal degradation of hemicelluloses and cellulose. Hemicelluloses typically decompose in the 160-360 °C range, while cellulose degrades at higher temperature, i.e., 240-390 °C [11]. However, a clear attribution of all the decomposition events or peaks to a specific chemical species appeared to be hardly achieved when analyzing the DTG profiles only, because mass losses of several minor chemical components probably occurred during each step at the same time.

3.2 Deconvoluted DTG curves

Deconvoluted DTG curves recorded at different heating rates are shown in Fig. 2 and the main corresponding separated peak data are listed in Table 2. Fig. 2 shows that the DTG curves were nicely fitted by Gaussian and Lorentzian Eq. (7) and (8). The percentage error of the fitted curves with respect to the experimental ones, as evaluated by the used deconvolution m-functions, was below 10 %. The number of deconvoluted peaks was found to depend on the heating rate. Specifically, the deconvolution procedure evidenced seven peaks at the lowest heating rate (i.e., 2 °C/min), eight peaks at medium heating rates (i.e., 5 and 10 °C/min) and nine peaks at higher heating rates (i.e., 20 and 40 °C/min). They simply correspond to the minimum number required to obtain a good superposition of the experimental profile and the fitting curve using Gaussian and Lorentzian line-shape functions. The use of symmetrical line-shape functions in fitting a real asymmetrical pattern typically requires more peaks than those actually present or visible as such or as shoulders in the real pattern [29].

3.3 Activation energies of tomato peels pseudo-components

On the basis of the above evidence, it was assumed that the pyrolysis of tomato peels is a multistage process modeled by assuming independent parallel reactions corresponding to the decomposition of seven pseudo-components termed as A, B, C, D, E, F, G, some of which being defined as double or sum peaks, as shown in Table 3 and marked in Fig. 2. To obtain the kinetics of each pseudo-component, the corresponding peaks were extracted from the overall differential thermogravimetric curves (DTG curve) recorded at the different heating rates (i.e., 2, 5, 10, 20, 40 °C/min) and were grouped together in Fig. 3. As expected, by increasing the heating rate, the DTG curves of almost all tomato peel pseudo-components are shifted to higher temperatures. The irregular peak shift with increasing heating rates, observed for pseudo-components F and G, is most likely a result of the observed effects of the heating rate on the TG curve shape, as described in *3.1 Thermogravimetric analysis*. The activation energies for each pseudo-component were obtained as a function of the conversion degree by using Friedman's isoconversional method, as described in the subsection *2.5.Pseudo-component kinetic analysis*. In order to exclude the errors inherent to the initial and the end periods, only the data in the range of $0.1 \leq \alpha \leq 0.90$ were considered. The regression analysis was performed by using SigmaPlot® software. The results obtained and the related correlation coefficient, R^2, which reflects the scattering of the experimental data used, are listed in Table 4.

It is worth noting that the apparent activation energies obtained for pseudo-components B and C were found consistent with the values reported in literature for hemicellulose (80-116 kJ/mol) and cellulose (195-286 kJ/mol), respectively [30, 31]. As a consequence, the peaks B and C may be associated with the thermal decomposition of hemicellulose and cellulose fractions, respectively. The E_α values of pseudo-components B and C also turned out in agreement with those obtained by Mangut et al. [5] for the single step decomposition of hemicellulose (116 MJ/mol) and for the two-step decomposition of cellulose (131 and 258 MJ/mol) from tomato peels. Again, it was found that the E_α values of pseudo-components D and E were consistent with those related to the first and second thermal decomposition stages of vegetable oils, e.g., from soybean, olive, canola and sunflower (78-107 kJ/mol and 209-349 kJ/mol) [32]. In addition, the E_α values of pseudo-components F and G matched those reported in literature for the lignin decomposition (29-49 kJ/mol) [33]. Accordingly, D and E peaks may be identified as two stages of the thermal decomposition of tomato peel oily fraction. Conversely, the pseudo-components F and G may be associated with the thermal decomposition of lignin. Anyhow, a lower matching was found for the E_α values obtained for pseudo-component D, E, F and G with those obtained by Mangut et al. [5] with regard to both the oily components (i.e., 176 and 209 MJ/kg) and the lignin fraction (i.e., 65, 135, 149, 162, 169, 173, 181 MJ/kg) of tomato peels.

Fig. 4a-b shows the dependence of the activation energy on the conversion degree for all the separated pseudo-components. Only the E_α-values which were found statistically significant, i.e. whose p-value was in the range of 0.01 to 0.1 [34], were considered. In more detail, it was found that almost all the E_α-values estimated for pseudo-components A, B, C, D, E and F were statistically significant at the 0.05 level (i.e., p-value lower than a significance level equal to 0.05), whereas those for pseudo-component G at the 0.1 level ($p\text{-value} < 0.1$). Data showed that the activation energies of the separated steps are almost all independent of the extent of conversion with an acceptable error, except those corresponding to pseudo-components B, C and E. In accordance with Vyazovkin et al. [8], this suggests that the thermal decomposition of pseudo-components B, C and E is not dominated by a single reaction step as it occurs to pseudo-components A, D, F and G. Principles and examples of a more in-depth mechanistic interpretation of the shape of E_α vs. α dependencies can be found elsewhere [7]. Error bars in Fig. 4a-b denote the 90% confidence interval (CI) for the estimated E_α-values, whose half-width was calculated by multiplying the standard error of the slope regression line by the appropriate 2-tailed critical value of the t-distribution having n-1 degrees of freedom for the error [35], where n is the number of data points. n was equal to 5 in this study, as a result of the five different heating rates considered for the kinetic analysis. It is worth nothing that, for a desired level of confidence, the higher the number of data points, the larger is the degree of freedom for the error, the lower is the critical value of the t-distribution [36] and the higher is the size of CI. Therefore, the width of the error bars in Fig. 4a-b reflect not only the uncertainty in the E_α but also the small number of data points used. The standard error of the slope regression line was as obtained directly by the SigmaPlot® software.

3.4 Validation of the kinetic approach

Fig. 5a-b shows the simulated and the experimental conversion curves of tomato peels under dynamic conditions at the constant heating rate of 60 and 80 °C/min, respectively. It can be observed that both curves obtained by the model simulations are an excellent reproduction of the experimental data, over the whole investigated temperature range. In particular, an average deviation percentage (AVP) as low as 1.8 % was obtained for the test at 60 °C/min by considering as many as 1900 experimental data points. Similarly, an average deviation percentage equal to 1.5 % was achieved for the simulation performed at 80 °C/min by considering about 1400 experimental data. Note that the different number of points in the two cases is simply the consequence of the shorter duration of the test at 80 °C/min for the same investigated temperature range. This obviously resulted in a lower number of experimental data.

4. Conclusion

The kinetics of the thermal decomposition of tomato peel residues in an inert atmosphere was investigated by non-isothermal thermogravimetric analysis at different heating rates (i.e., 2, 5, 10, 20, 40 °C/min). Thermogravimetric measurements highlighted that the pyrolysis of the investigated tomato processing residue is a rather complex process that occurs in several simultaneously running stages with overlapping peaks. Due to the complexity of the investigated process, an analytical approach involving the deconvolution of the overlapping decomposition steps from the overall differential thermogravimetric curves by using conventional symmetric functions (i.e., the

Lorentzian and Gaussian ones) and the subsequent application of model-free kinetic methods to the separated peaks, was adopted. Seven pseudo-components were identified as a result of the deconvolution procedure and satisfactorily associated with the main constituents of the investigated tomato peels. The Friedman's isoconversional method was employed to evaluate the dependence of the activation energy on the extent of conversion for individual pseudo-components resulting from the deconvolution procedure. The computed kinetic parameters proved to be suitable for the prediction of the behavior of the sample over the range of the dynamic heating conditions at which the same parameters were determined, i.e. 2-40 °C/min. The check on the prediction ability of the evaluated kinetic parameters was carried out through an extrapolation to the heating of 60 and 80 °C/min. Simulated and experimental data showed an excellent agreement over the whole investigated temperature range (i.e., average deviation percentage lower than 2 %), indicating that the computed kinetic parameters could be used for modeling and design of torrefaction and pyrolysis processes involving the investigated tomato residues.

5. Acknowledgement

This work has been carried out in the frame of the "Training on the job" project (Dottorato in Azienda) funded by the Campania Region. The role and the interest of the Magaldi Power SpA as a hosting company in this project are highly acknowledged.

The authors are grateful to the Prof. Vincenzo Palma of the University of Salerno for providing expertise and access to their TGA facilities. Special thanks to Dr. Daniela Barba for the valuable support in performing the TG-DTG analyses.

The authors are also thankful to Prof. Marisa Di Matteo for providing samples of tomato residues within the "Tom & Cherry" National Research Project (PON).

References

[1] Tomato news. Tomato processing Industry, 2014. Available online at: http://www.tomatonews.com/resources.html (Accessed June 26, 2015).

[2] A.A.A. Al Khraisat, Evaluation of metabolizable nutrient values of Tomato Pomace (TP) in Nile tilapia (Oreochromis niloticus), Int. J. Fisc. Aquat. Sci. 2 (2015) 164-167.

[3] P. Brachi, F. Miccio, M. Miccio, G. Ruoppolo, Fluidized bed torrefaction of industrial tomato peels: set-up of a new batch lab-scale test rig and preliminary experimental results. Proceedings of the 22nd International Conference of Fluidized Bed Conversion, Turku, Finland, ISBN 978-952-12-3222-0, pp. 438-447, June 14-17, 2015.

[4] G. Toscano, A. Pizzi, E. Foppa Pedretti, G. Rossini, G. Ciceri, G. Martignon, D. Duca, Torrefaction of tomato industry residues, Fuel 143 (2015) 89-97.

[5] V. Mangut., E. Sabio, J. Ganàn, J.F. Gonzalez, A. Ramiro, C.M. Gonzàlez, S. Romànan, A. Al-Kassir, Thermogravimetric study of the pyrolysis of biomass residues from tomato processing industry, Fuel Process. Technol. 87 (2006) 109-115.

[6] E. Sabio, A. Álvarez-Murillo, S. Román, B. Ledesma, Conversion of tomato-peel waste into solid fuel by hydrothermal carbonization: Influence of the processing variables, Waste Manage. (2015) IN PRESS.

[7] S. Vyazovkin, C.A. Wight, Isothermal and non-isothermal kinetics of thermally stimulated reactions of solids, Inter. Rev. Phys. Chem. 17 (1998) 407-433.

[8] S. Vyazovkin, A.K. Burnham, J.M. Criado, L.A. Pérez-Maqueda, C. Popescu, N Sbirrazzuoli, ICTAC Kinetics Committee recommendations for performing kinetic computations on thermal analysis data, Thermochim. Acta 520 (2011) 1-19.

[9] P. Brachi, F. Miccio, M. Miccio, G. Ruoppolo, Isoconversional kinetic analysis of the olive pomace decomposition under torrefaction operating conditions, Fuel Process. Technol. 30 (2015) 147-154.

[10] H.L. Friedman, Kinetics of thermal degradation of char-forming plastics from thermogravimetry. Application to a phenolic plastic, J. Polym. Sci. Pol. Sym. (1964) 183-195.

[11] A.O. Aboyade, T. J. Hugoa, Marion Carrier, E.L. Meyer, R. Stahl, J. H. Knoetze, J. F. Görgens, Non-isothermal kinetic analysis of the devolatilization of corn cobs and sugar cane bagasse in an inert atmosphere, Thermochim. Acta, 517 (2011) 81-89.

[12] E. Moukhina, Determination of kinetic mechanisms for reactions measured with thermoanalytical instruments, J. Therm. Anal. Calorim. 109 (2012) 1203-1214.

[13] S. Vyazovkin, N. Sbirrazzuoli, Isoconversional kinetic analysis of thermally stimulated process in polymers, Macromolecular Rapid Communications 27 (2006) 1515–1532.

[14] M. Venkatesh, P. Ravi, S.P. Tewari, Isoconversional kinetic analysis of decomposition of nitroimidazoles: Friedman method vs Flynn–Wall–Ozawa method, Journal of Physical Chemistry A 117 (2013) 10162–10169.

[15] R.M. Rowell, Handbook of wood chemistry and wood composites, first ed., Taylor and Francis Group, CRC Press, FL, USA, 2005.

[16] B. Hames, R.Ruiz, C. Scarlata , A. Sluiter, J. Sluiter, D.Templeton, Preparation of samples for compositional analysis. Laboratory Analytical Procedure (LAP). NREL/TP-510–42620. National Renewable Energy Laboratory, Golden, Colorado, 2008.

[17] H. Chen, W. Zhao, N. Liu, Thermal Analysis and Decomposition Kinetics of Chinese Forest Peat under Nitrogen and Air Atmospheres, Energ. Fuel 25 (2011) 797–803.

[18] Available online at: http://it.mathworks.com/matlabcentral/fileexchange/?s_tid=gn_mlc_fx (Accessed December 19, 2015).

[19] G.E. Urroz, Numerical Solution to Ordinary Differential Equations (2014). Available online at: http://ocw.usu.edu/Civil_and_Environmental_Engineering/Numerical_Methods_in_Civil_Engineering/ODEsMatlab.pdf (Accessed March 2, 2016).

[20] S. Viazovkyn, A unified approach to kinetic processing of nonisothermal data, Int. J. Chem. Kinet. 28 (1996) 95-101.

[21] J.J.M. Orfao, F.J.A. Antunes, J.L. Figueiredo, Pyrolysis kinetics of lignocellulosic materials-three independent reactions model, Fuel 78 (1999) 349-358.

[22] C. Vasile, C.M, Popescu, M.C. Popescu, M. Brebu, S. Willfor, Thermal behaviour/treatments of some vegetable residues. IV. Thermal decomposition of eucalyptus wood, Cellulose Chem. Technol. 45 (2011) 29-42.

[23] J. Sun, W. Wang, Z. Liu, Q. Ma, C. Zhao, C. Ma, Kinetic Study of the Pyrolysis of Waste Printed Circuit Boards Subject to Conventional and Microwave Heating, Energies 5 (2012) 3295-3306.

[24] Y. Leng, Materials Characterization: Introduction to Microscopic and Spectroscopic Methods, John Wiley & Sons (Asia) Pte Ltd, Singapore, 2008.

[25] V. Strezov, J.A. Lucas, T.J. Evans, L. Strezov, Effect of heating rate on the thermal properties and devolatilisation of coal, J. Therm. Anal. Calorim. 78 (2004) 385–397.

[26] C. Gomez, E. Velo, F. Barontini, V. Cozzani, Influence of Secondary Reactions on the Heat of Pyrolysis of Biomass, Ind. Eng. Chem. Res. 48 (2009) 10222–10233.

[27] E.S. Lazos, P. Kalathenos, Technical Note: Composition of tomato processing wastes, Int. J. Food Sci. Tech. 23(1988) 649-652.

[28] M. Knoblich, B. Anderson, D. Latshaw, Analyses of tomato peel and seed byproducts and their use and a source of carotenoids, J. Sci. Food Agric. 85(2005) 1166-1177.

[29] T. O'Haver, A Pragmatic Introduction to Signal Processing. Available online at: https://terpconnect.umd.edu/~toh/spectrum/CurveFittingC.html (Accessed February 23, 2016).

[30] C. Branca, A. Albano, C. Di Blasi, Critical evaluation of global mechanisms of wood devolatilization, Termochim. Acta 429 (2005) 133-141.

[31] M.G. Gronli, G. Varhegyi, C. Di Blasi, Thermogravimetric analysis and devolatilization kinetics of wood, Ind. Eng. Chem. Res. 41 (2002) 4201-4208.

[32] J.C. Oliveira Santos, J.P. Dantas, A. Gouveia de Souza, M.M. da Conceição, Kinetic parameters on thermal degradation of edible vegetable oils by thermogravimetric data. Proceeding of the II Congresso Brasileiro de Plantas Oleaginosas, Óleos, Gorduras e Biodiesel. Available at: http://oleo.ufla.br/anais_02/artigos/t007.pdf (Accessed February 28, 2016).

[33] X.Y. Wang, X.J. Wan, M.Q. Chen, J. Wang, Kinetic model of biomass pyrolysis based on three-component independent parallel first-order reactions, Chinese J. Chem. Eng. 12 (2012) 1020-1024.

[34] M. Baron, Probability and Statistics for Computer Scientists, Second Edition, CRC Press, Boca Raton, London (2013).

[35] M.A. Rosenblum, M. J. van der Laan, Confidence Intervals for the Population Mean Tailored to Small Sample Sizes, with Applications to Survey Sampling, Int. J. Biostat. 5 (2009) 1-44.

[36] Available online at: https://www.medcalc.org/manual/t-distribution.php (Accessed February 4, 2016).

Table 1. – Raw tomato peel properties.

Moisture (wt.%, as received)	80.50 ± 0.01
Proximate analysis (wt.%, dry basis)	
Volatile Matter	84.34 ± 0.09
Fixed Carbon	13.40 ± 0.06
Ash	2.3 ± 0.1
Ultimate analysis (wt.%, dry basis)	
C	55.9 ± 0.5
H	8.2 ± 0.3
N	1.4 ± 0.1
S	0.05 ± 0.01
O (by diff.)	34.5 ± 0.6
Calorific value analysis (MJ/kg, dry basis)	
HHV	24.7 ± 0.6
LHV	23.8 ± 0.6
Polymeric composition (wt.%, dry basis)	
Extractive	5.2 ± 0.1
Hemicellulose	52.4 ± 0.1
A-cellulose	17.5 ± 0.1
Lignin (by difference)	24.9 ± 0.2

Table 2 – Characteristics of deconvoluted peaks of DTG curves recorded at different heating rates.

Heating rate (°C/min)	No. of peaks	Peak 0		Peak 1		Peak 2		Peak 3		Peak 4		Peak 5		Peak 6		Peak 7		Peak 8	
		x_o	S	x_o	S	x_o	S	x_o	S	x_o	S	x_o	S	x_o	S	x_o	S	x_o	S
2	7	43.57	13	216.5	12	298.5	71	344.5	37	427.7	33	480.0	30	513.5	16	-	-	-	-
5	8	50.22	30	228.5	65	314.8	127	361.8	127	433.0	24	447.3	63	520	79	576.0	25	-	-
10	8	65.4	44	240.0	95	326.8	332	373.9	73	402.3	116	452.0	127	570.0	145	760	80	-	-
20	9	71.0	137	249.0	300	340.0	633	391.5	141	422.5	300	463.5	225	587	142	760	70	950	250
40	9	79.0	190	257	680	354.5	950	411.0	800	441.4	805	479.5	350	700.0	146	799.8	65	970.1	400

x_o (°C)
S (%wt./min·°C)

Table 3 –Pseudocomponents and deconvoluted peak association.

Heating rate (°C/min)	A	B	C	D	E	F	G
2	Peak 0	Peak 1	Peak 2	Peak 3	Peak 4	Peak 5	Peak 6
5	Peak 0	Peak 1	Peak 2	Peak 3	Peaks 4 + 5	Peak 6	Peak 7
10	Peak 0	Peak 1	Peak 2	Peaks 3 + 4	Peak 5	Peak 6	Peak 7
20	Peak 0	Peak 1	Peak 2	Peaks 3 + 4	Peak 5	Peak 6	Peak 7
40	Peak 0	Peak 1	Peak2	Peaks 3 + 4	Peak 5	Peak 6	Peak 7

Table 4 – Activation energies of the decomposition of tomato peels pseudo-components by Friedman's isoconversional method.

Pseudocomponent	**A**		**B**		**C**		**D**		**E**		**F**		**G**	
α (-)	**E(kJ/mol)**	**R^2**	**Eα(kJ/mol)**	**R^2**	**E(kJ/mol)**	**R^2**	**E(kJ/mol)**	**R^2**	**E(kJ/mol)**	**R^2**	**E(kJ/mol)**	**R^2**	**E(kJ/mol)**	**R^2**
0.1	94.84	0.90	77.29	0.44	107.88	0.98	99.68	0.88	210.12	0.96	50.99	0.84	30.89	0.47
0.15	87.89	0.93	150.86	0.84	124.14	0.99	112.63	0.96	227.86	0.99	55.06	0.91	29.53	0.46
0.2	83.58	0.95	159.98	0.98	135.90	1.00	117.36	0.99	236.64	0.99	56.26	0.94	28.51	0.44
0.25	80.87	0.96	147.87	0.99	145.06	1.00	116.80	0.99	241.63	0.99	55.95	0.94	27.65	0.43
0.3	78.30	0.97	138.26	0.99	152.54	1.00	113.02	0.99	245.92	0.99	54.83	0.92	26.95	0.42
0.35	77.43	0.98	131.70	0.98	159.15	1.00	108.21	0.99	256.66	0.99	53.24	0.90	26.33	0.41
0.4	76.81	0.98	126.56	0.98	164.97	1.00	104.32	0.99	256.66	1.00	51.45	0.87	25.80	0.41
0.45	76.80	0.98	120.95	0.98	170.7	1.00	102.43	0.99	263.02	1.00	49.50	0.84	25.29	0.40
0.5	78.12	0.98	115.30	0.97	175.96	1.00	103.05	0.99	267.95	1.00	47.52	0.81	24.81	0.39
0.55	79.47	0.97	109.00	0.96	181.09	0.99	105.08	0.99	271.79	1.00	45.54	0.77	24.36	0.39
0.6	82.19	0.96	101.37	0.94	187.40	0.99	107.92	0.99	273.49	1.00	43.53	0.74	23.92	0.38
0.65	85.24	0.94	91.83	0.90	194.28	0.98	111.06	0.99	276.75	0.99	41.58	0.71	23.49	0.38
0.7	90.19	0.91	80.77	0.82	200.85	0.98	114.08	0.99	278.51	0.99	39.61	0.68	23.03	0.37
0.75	96.10	0.84	58.46	0.68	210.70	0.96	116.36	0.98	283.75	0.99	37.57	0.65	22.60	0.36
0.8	102.69	0.71	48.41	0.47	224.10	0.94	118.37	0.97	290.74	0.98	35.45	0.61	22.16	0.36
0.85	93.01	0.41	27.43	0.20	240.71	0.89	120.35	0.95	297.05	0.96	33.34	0.58	21.58	0.35
0.9	9.67	0.01	4.41	0.01	261.98	0.77	123.28	0.91	308.06	0.94	30.93	0.54	21.02	0.34

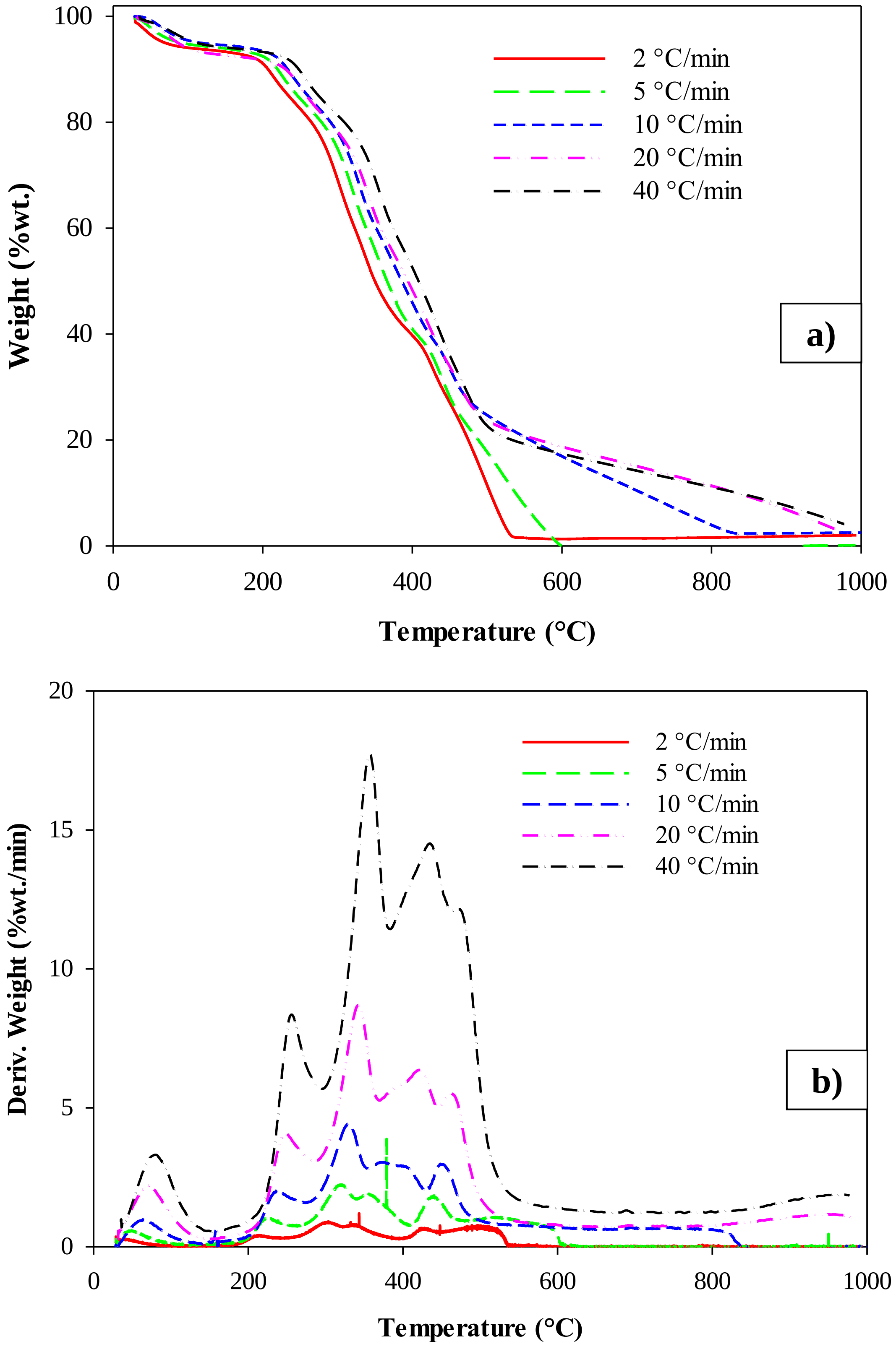

Fig. 1 Tomato peels (a) TG and (b) DTG curves at different heating rates (2, 5, 10, 20, 40 °C/min) recorded in nitrogen atmosphere with a purge rate of 100 ml/min from ambient temperature to about 1000 °C.

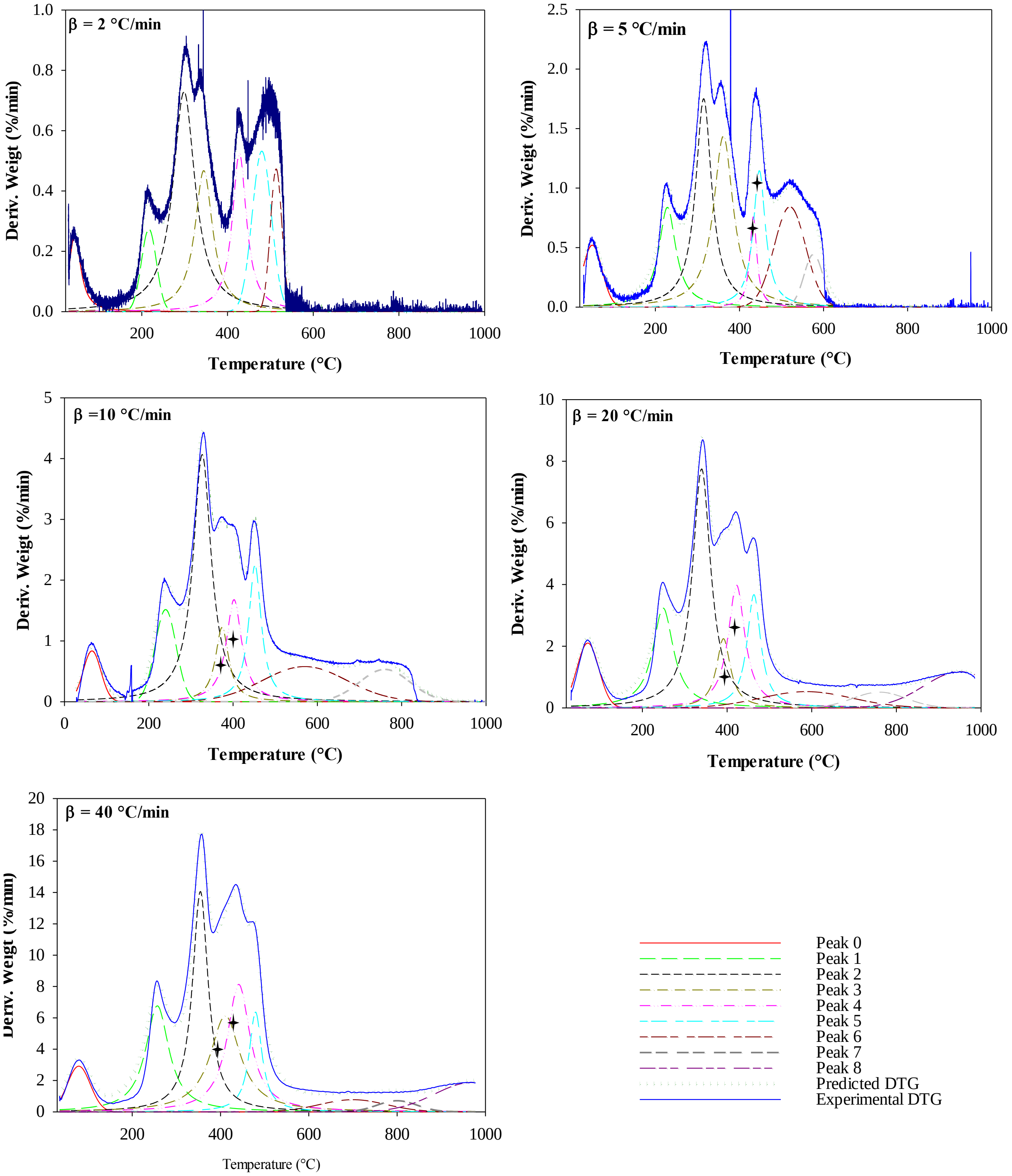

Fig. 2 Deconvoluted vs. original DTG curves recorded at heating rates of 2, 5, 10, 20, 40 °C/min for tomato peel samples. Symbol† marks the merged peaks.

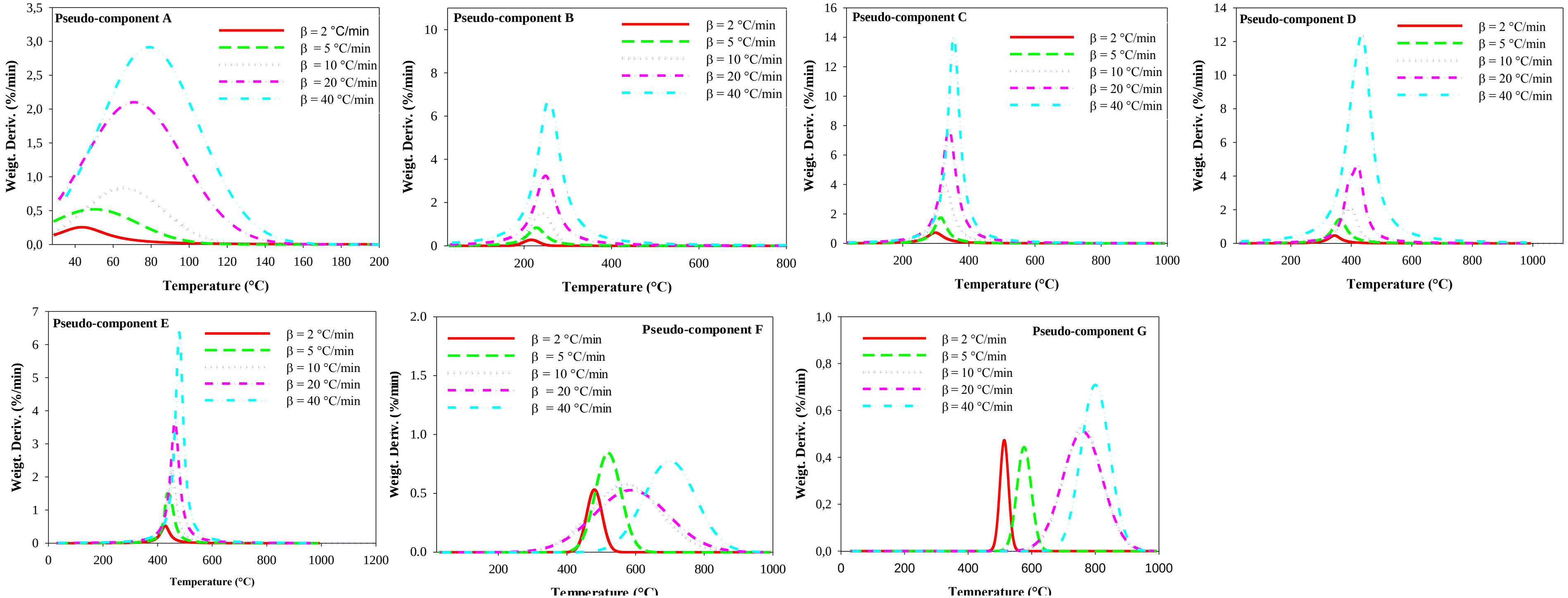

Fig. 3 DTG of tomato peels pseudo-components obtained by the deconvolution of global DTG curves recorded at different linear heating rates (2, 5, 10, 20, 40 °C/min).

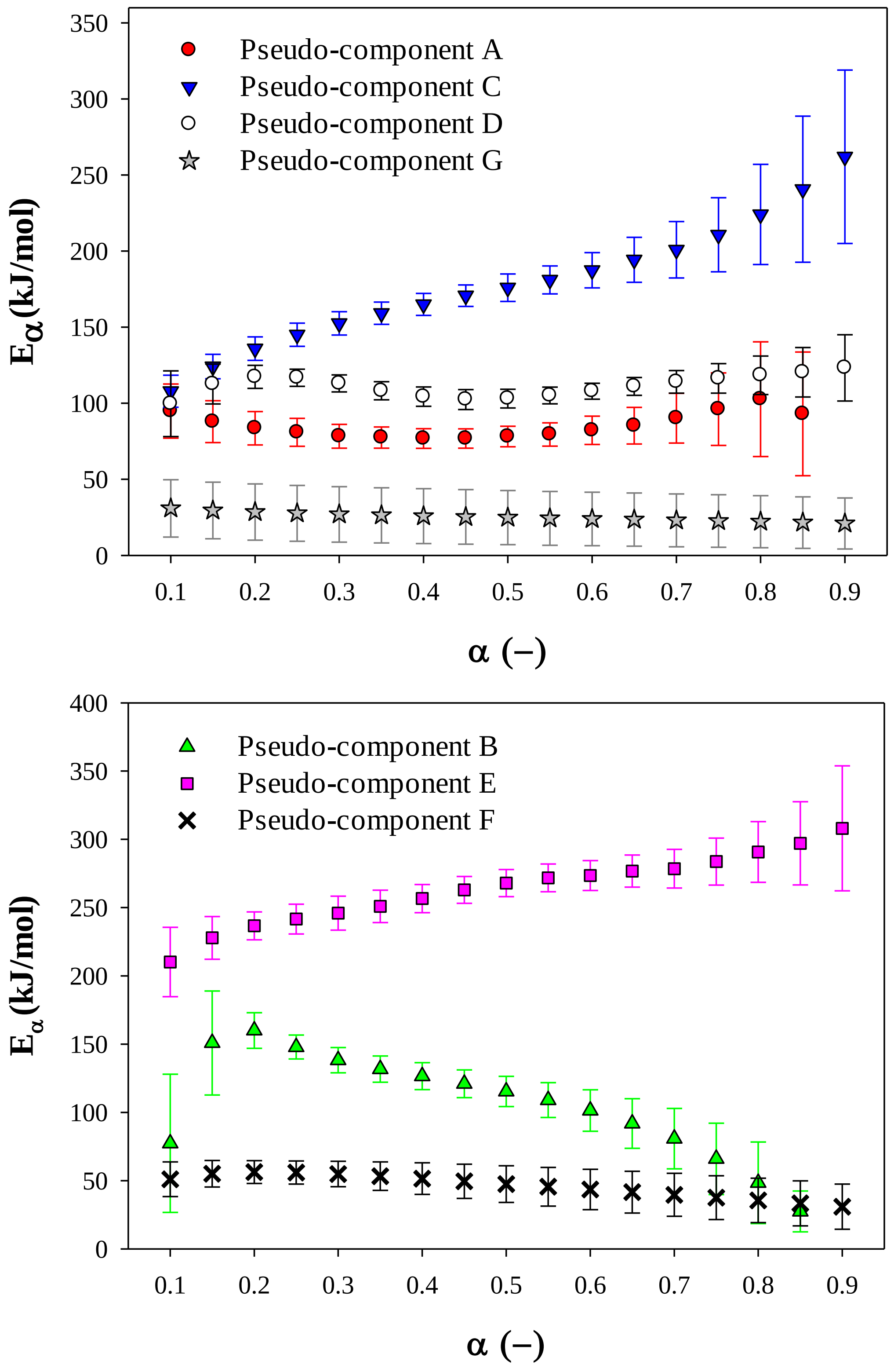

Fig. 4 Activation energy dependence for tomato peels pseudo-components. Graphs were grouped so as to reduce the overlap of error bars.

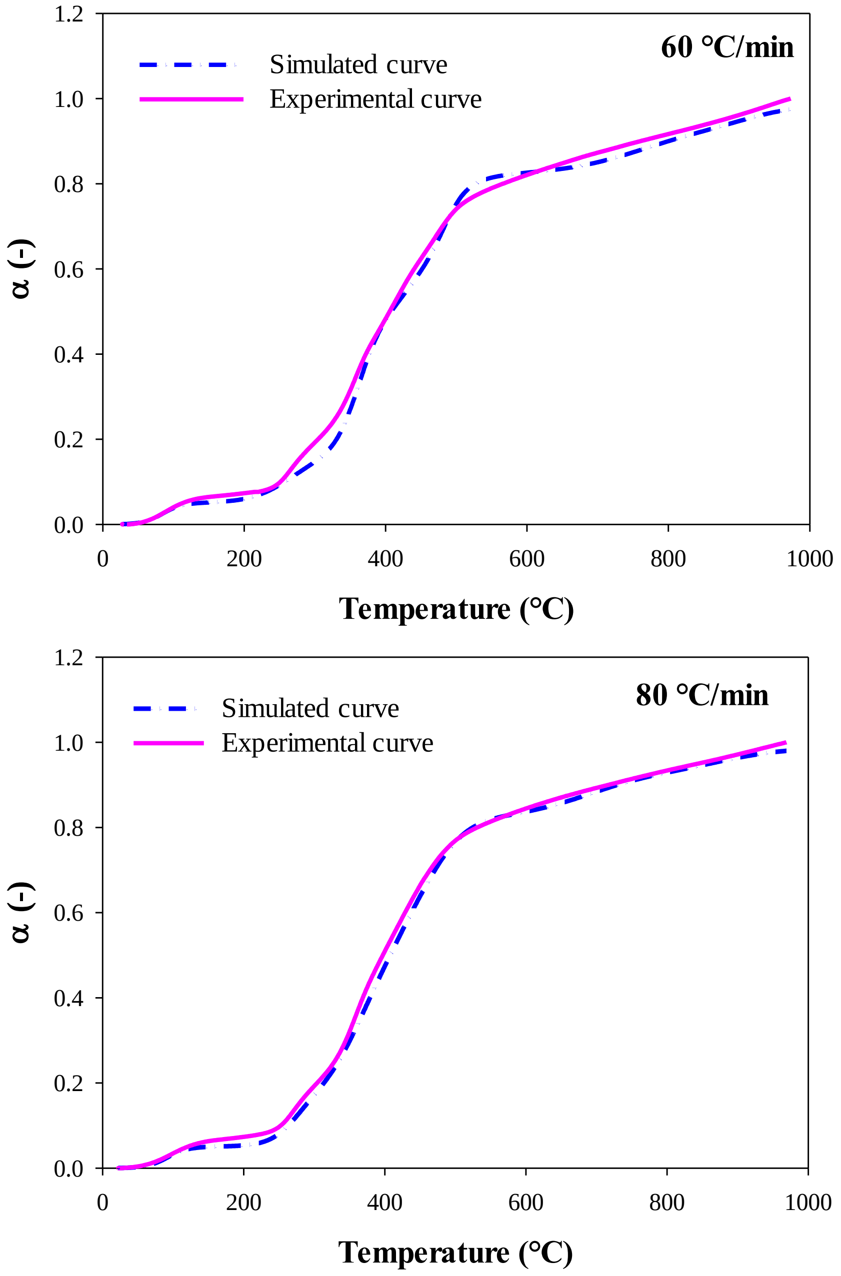

Fig. 5 Experimental and simulated tomato peel conversion curve under dynamic conditions at a constant heating rate of 60 and 80 °C/min.